

# Confinement dependence on $\beta$ /power in the JET ILW hybrid scenario

**J. Hobirk**<sup>1</sup>, C. Angioni<sup>1</sup>, C. D. Challis<sup>2</sup>, O. J. W. F. Kardaun<sup>1</sup>, A. Kappatou<sup>1</sup>, E. Lerche<sup>3</sup>, M. Maslov<sup>2</sup>, F. Ryter<sup>1</sup> and JET contributors\*

EUROFusion Consortium JET, Culham Science Centre, OX14 3DB, Abingdon, UK

<sup>1</sup> Max-Planck-Institut für Plasmaphysik, Boltzmannstr. 2, 85748 Garching

<sup>2</sup> UKAEA, Culham Science Centre, Abingdon, Oxon, OX14 3DB, UK

<sup>3</sup> Laboratory for Plasma Physics, LPP-ERM/KMS, B-1000 Brussels, Belgium

The hybrid scenario on JET can have an improved confinement compared to the IPB98(y,2) scaling prediction[1]. This has been observed before on many other experiments, e.g. DIII-D

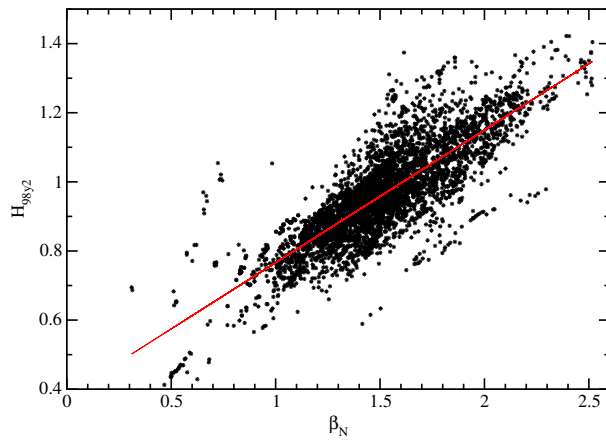


Figure 1: Scatter plot of  $H_{98,y2}$  and  $\beta_N$  in DB

and AUG. From a scaling point of view it is a very interesting question whether this confinement improvement is a consequence of the higher beta operation in the hybrid scenario compared to the traditional H-mode [2] or if the higher normalised confinement is e.g. due to a weaker power degradation as reported in [3]. The H-factor and the plasma  $\beta_N$  are derived both from the stored energy and hence tend to be strongly correlated (see in figure 1 a plot like in [2] for the database used in this paper).

In an attempt to disentangle  $\beta$  and H-factor a database (DB) analysis of about 4500 points from the entire JET ITER-like wall period has been performed. Here deuterium, pulses done as part of the hybrid scenario development in a low triangularity lower single null shape are

	$\ln(I_p)$	$\ln(B_T)$	$\ln(n_e)$	$\ln(P_{\text{loss}})$	$\ln(\Gamma)$	$\ln(\beta_p)$	$\ln(\beta_N)$
$\ln(I_p)$	1	<b>0.91</b>	<b>0.88</b>	<b>0.78</b>	0.46	-0.26	-0.21
$\ln(B_T)$		1	<b>0.77</b>	<b>0.83</b>	0.44	-0.09	-0.34
$\ln(n_e)$			1	<b>0.76</b>	0.45	-0.14	-0.005
$\ln(P_{\text{loss}})$				1	0.367	0.28	0.10
$\ln(\Gamma)$					1	-0.29	-0.27
$\ln(\beta_p)$						1	<b>0.7</b>

Table 1: Correlation matrix

included. The database is large and diverse with a wide  $\beta$  range ( $0.5 < \beta_N < 2.7$ ), it covers the following ranges in the main scaling parameters:  $0.8\text{MA} < I_p < 3\text{MA}$ ,  $1\text{T} < B_T < 4\text{T}$ ,  $2\text{MW} < P_{\text{loss}} < 38\text{MW}$  dominantly NBI,  $2 \cdot 10^{19}\text{m}^{-3} < n_e < 7 \cdot 10^{19}\text{m}^{-3}$ . The variation of the geometry factors in the DB is very small. In table 1 the correlation matrix of the main scaling parameters is shown. The scenario has been mainly developed for low density, high  $\beta_N$  plasmas at mostly constant  $q_{95}$ . Hence  $I_p$ ,  $B_T$ ,  $n_e$  and  $P_{\text{loss}}$  are strongly correlated. One consequence of this are large uncertainties in the scaling exponents if this database would be used to derive a new scaling.

\*See the author list of J. Mailloux et al., 2022 Nucl. Fusion, <https://doi.org/10.1088/1741-4326/ac47b4>

Instead in this paper we use the database to check if existing scalings are consistent with the data in this DB.

This analysis has been done either assuming IPB98(y,2)[5]<sup>†</sup> or ITPA 20 – ITER like (IL20 from now on) [4]<sup>‡</sup> scaling properties. In figure 2 the H-factor the data points have been normalised to  $P_{\text{loss}}^{-0.69}$  and then being plotted against  $P_{\text{loss}}$ . The data has been marked in different

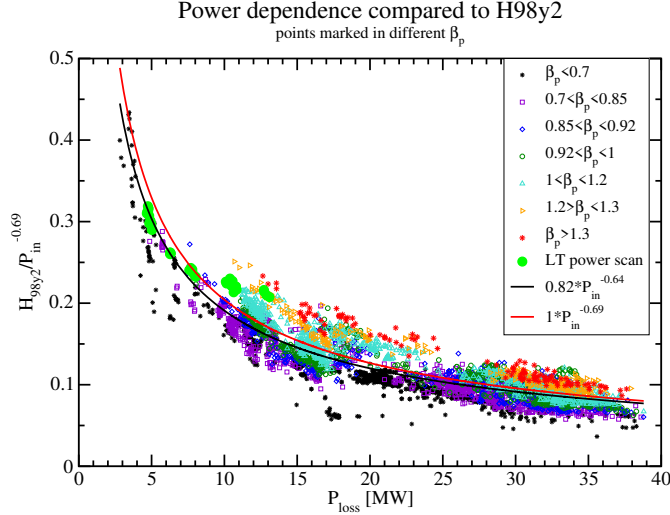


Figure 2:  $P_{\text{loss}}$  versus  $H_{98y2}$ -factor normalised to  $P_{\text{loss}}^{-0.69}$ . The observed variation orders apparently with  $\beta_{\text{pol}}$ , the black points being the lowest the red points are the highest. Thirdly, the green marked power scan follows indeed a different trajectory and apparently “breaks” the IPB98(y,2) prediction but the points are within the variations within the DB and follow the observed trend in  $\beta_{\text{pol}}$ . A similar figure can be obtained using  $\beta_N$  as ordering parameter, just at very high heating power, which was dominantly used at higher  $q_{95}$ , the ordering is not as good.

If only a subset of the data in a reduced beta range for medium beta is considered, the same agreement is found as shown in figure 3. On the left hand side the data with  $\beta_{\text{pol}} < 0.7$  and the

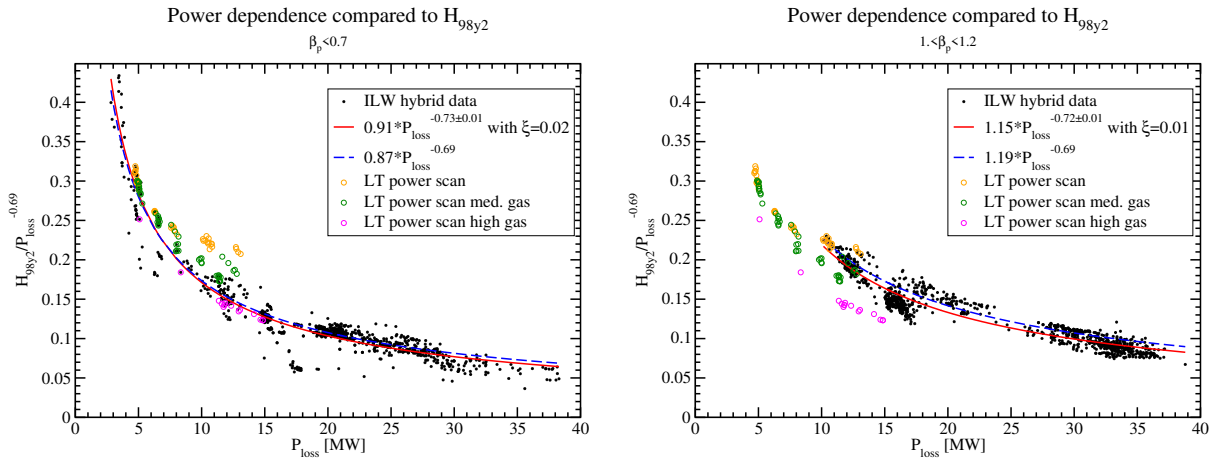


Figure 3:  $P_{\text{loss}}$  dependence of  $H_{98y2}$  at different  $\beta_{\text{pol}}$  corresponding fits are shown. Also a fit using the IPB98(y,2) scaling exponent has been added in blue. The multiplier in this case acts as a confinement multiplier (same in figure 5). The exponent of the fit to the data is slightly larger than IPB98(y,2). As additional points on the plot the power scan from [3] and its repeat at medium and high gas are added. Those points correspond more to the scaling law power degradation and indicate that gas injection rate could

<sup>†</sup>  $\tau_E^{\text{IPB98(y,2)}} = 0.056 \cdot I_p^{0.93} B_T^{0.15} P_{\text{loss}}^{-0.69} \bar{n}_e^{0.41} M^{0.19} R^{1.39} a^{0.58} k^{0.78}$

<sup>‡</sup>  $\tau_E^{\text{ITPA 20IL}} = 0.067 \cdot I_p^{1.29} B_T^{0.13} P_{\text{loss}}^{-0.644} \bar{n}_e^{0.147} M^{0.30} R^{1.19} (1 + \delta)^{0.56} \kappa_a^{0.67}$

be a hidden parameter in this DB. Please be aware that those points are only considered for the fit if they are in the right beta range (should have a black dot inside). This very low beta range is overlaying largely with the points at high gas even though most of the points have low beta without having a high gas injection. On the right side the same plot is shown for a higher  $\beta_{\text{pol}}$  range. The fitted exponent is again slightly higher than IPB98(y,2). The multiplier in front of the IPB98(y,2) scaling had to increase considerably to be a reasonable representation of the data. Please note that the scatter is still significant.

The ordering in  $\beta_{\text{pol}}$  within the plot against  $P_{\text{loss}}$  could of course be a consequence of a deviation in other scaling parameters or of parameters which are not included in the scaling law (hidden variables). In figure 4 on the left hand side the DB as a function of  $B_T$  and on the right hand side as a function of  $\bar{n}_e$  is shown. The fits to the DB are close to the ones in the

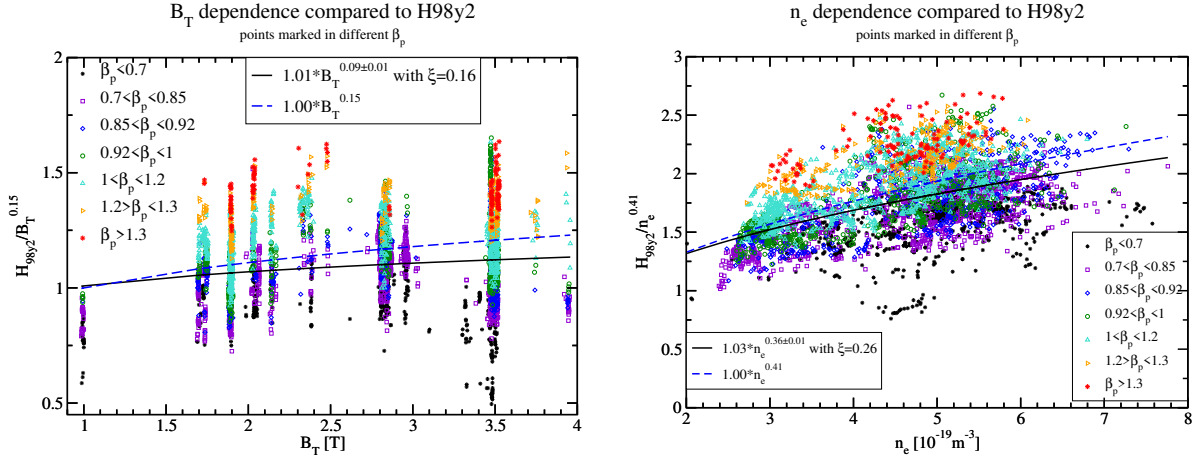


Figure 4: DB scatter plot as function of  $B_T$  and  $\bar{n}_e$

IPB98(y,2). Often it is observed that the normalised confinement degrades as the density is increased. In this database the density variations are mainly due to  $I_p$ /confinement variations and not excessive gas injection. This might explain why the density dependence so close to IPB98(y,2). As expected the scatter is very high again and the points are ordered again in  $\beta_{\text{pol}}$ . No significant deviation from the IPB98(y,2) scaling is observed in those 2 parameters. The  $I_p$  dependence is also close to IPB98(y,2) (not shown here).

As a further test, the scaling law has been changed to the IL20 properties which results in a better global agreement (not shown here) but also a large scatter is visible which orders similarly in  $\beta_{\text{pol}}$ . The exponents of this scaling fit very well to the low beta part of the DB. In figure 5 the upper left graph shows excellent agreement between the data, the IL20 scaling and the fit to the data. On the other hand, the graph in the upper right shows that at medium beta a less strong power degradation  $P_{\text{loss}}^{0.55}$  would fit better to this part of the DB. In the lower part of figure 5 the exponent of the fit as a function of  $\beta_{\text{pol}}$  is plotted for  $P_{\text{loss}}$  (left),  $B_T$  (middle) and  $\bar{n}_e$  (right) for the IPB98(y,2) scaling in black and the IL20 scaling in red. It is observed that at the lowest  $\beta_{\text{pol}}$  the exponent of the fit corresponds very well to the IL20 dependence (ref dashed line). Over some beta range the exponent deviates significantly from the IL20 scaling and for the  $\bar{n}_e$  dependence there is a clear tendency to go back to the IPB98(y,2) scaling value (black dashed). Also the  $B_T$  exponents come closer to IPB98(y,2) and one can speculate that the apparent reduced power degradation could be a consequence of the changed  $B_T$  dependence coupled by beta. At the highest beta the exponent tends to go back to the IL20 scaling prediction but the available data in this region maybe insufficient to draw a precise conclusion. The dependence of the exponent on beta might indicate that the low beta and confinement part of the DB, which is closer to the traditional H-mode operating space, indeed scales more like

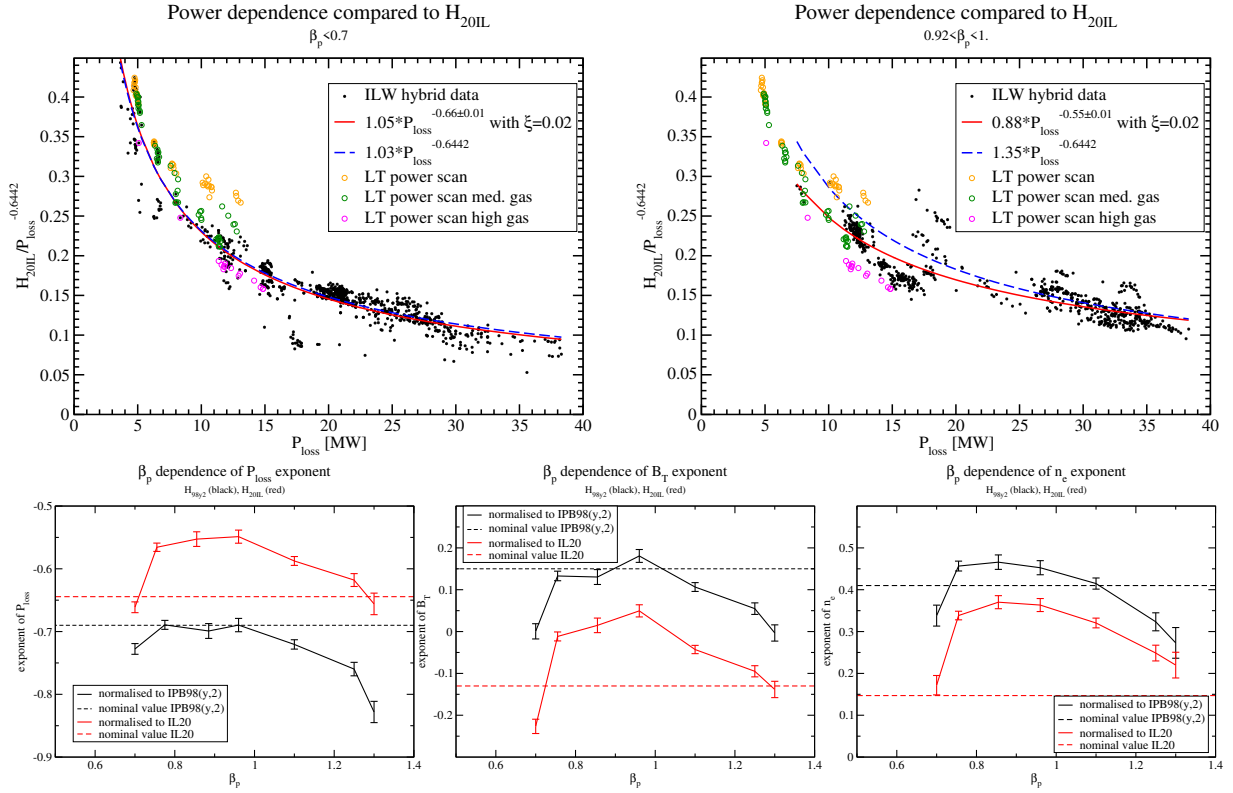


Figure 5: DB at different  $\beta_{pol}$  compared to IL20

IL20, whereas the more hybrid like operation space (lower gas fluxes and higher input power) scales more like IPB98(y,2).

The observed deviations compared to the IL20 scaling assumption re-enforces the finding of the good agreement especially with the  $P_{loss}$  (but also  $\bar{n}_e$ ) dependence of the IPB98(y,2) scaling law despite the better general agreement with the IL20 like scaling. The driving factor of the confinement dependence seems not to be a weaker power degradation but an increase of confinement with beta which is not captured by the other engineering regression variables and would likely require additional variables or a different functional dependence, e.g. offset-linear or log non-linear scalings. In general these findings might be explained by the observed better pedestal stability and lower turbulence growth rates at higher beta as also been indicated in [3].

## Acknowledgement

This work has been carried out within the framework of the EUROfusion Consortium, funded by the European Union via the Euratom Research and Training Programme (Grant Agreement No 101052200 — EUROfusion). Views and opinions expressed are however those of the author(s) only and do not necessarily reflect those of the European Union or the European Commission. Neither the European Union nor the European Commission can be held responsible for them.

## References

- [1] J. Hobirk *et al.*, PPCF **54**, 095001, (2012).
- [2] M. Beurskens *et al.*, PPCF **55**, 124043, (2013).
- [3] C. D. Challis *et al.*, NF **55**, 053031, (2015).
- [4] G. Verdoolaege *et al.*, NF **61**, 076006, (2021).
- [5] ITER Physics Basis, Editors, NF **39**, 2137, (1999).